Nonconservative and reverse spectral transfer in Hasegawa–Mima turbulence

P. W. Terry and D. E. Newman
Department of Physics, University of Wisconsin–Madison, Madison, Wisconsin 53706

(Received 27 January 1993; accepted 29 March 1993)

The dual cascade is generally represented as a conservative cascade of enstrophy to short wavelengths through an enstrophy similarity range and an inverse cascade of energy to long wavelengths through an energy similarity range. This picture, based on a proof due to Kraichnan [Phys. Fluids **10**, 1417 (1967)], is found to be significantly modified for spectra of finite extent. Dimensional arguments and direct measurement of spectral flow in Hasegawa–Mima turbulence indicate that for both the energy and enstrophy cascades, transfer of the conserved quantity is accompanied by a nonconservative transfer of the other quantity. The decrease of a given invariant (energy or enstrophy) in the nonconservative transfer in one similarity range is balanced by the increase of that quantity in the other similarity range, thus maintaining net invariance. The increase or decrease of a given invariant quantity in one similarity range depends on the injection scale and is consistent with that quantity being carried in a self-similar transfer of the other invariant quantity. This leads, in an inertial range of finite size, to some energy being carried to small scales and some enstrophy being carried to large scales.

I. INTRODUCTION

Spectral transfer of energy and other dynamical invariants, such as the enstrophy, or mean-squared vorticity,[1,2] has long been considered an important aspect of turbulence. In particular, the nature and direction of spectral energy transfer has direct bearing on the way in which instability-driven turbulence is saturated, on the magnitude and shape of the spectrum, and ultimately on the nature of spatial transport produced by the turbulence.

A number of recent studies underscore the importance of spectral transfer.[3–5] For example, it has recently been shown from closure theory[6] and direct measurement of spectral transfer rates in numerically integrated model equations,[3] that dissipative trapped ion convective cell turbulence transfers energy from the long wavelengths of the driving instability to shorter wavelengths. This result has invalidated prior dogma which held that dissipative trapped ion convective cells would transfer energy to longer wavelengths, producing extremely large cell sizes and catastrophic transport. In related studies of broadband dissipative trapped electron mode turbulence,[4,5] it has been found that the spectral transfer evinces two distinct subranges at long and short wavelength extremes, separated by a highly complex intermediate subrange. In the long wavelength subrange, energy is transferred to small scales in a process that is distinctly anisotropic and nonlocal in wave-number space. Significant production of enstrophy accompanies the transfer to shorter wavelength. In the short wavelength subrange, nonlinear transfer very nearly conserves enstrophy. The constraint of two conserved quadratic quantities (energy and enstrophy) gives rise to an isotropic, local-in-wave-number space dual cascade with some energy flowing back toward the long wavelength subrange and enstrophy flowing toward shorter scales. These spectral transfer properties produce a distinctive energy spectrum shape $E(k_x,k_y)$, with a flat elliptical plateau in the long wavelength subrange and a falloff beyond in the short wavelength subrange.[4]

The dual cascade observed in the short wavelength subrange of dissipative trapped electron mode turbulence is a manifestation of a transfer process first identified in two-dimensional (2-D) Navier–Stokes turbulence (and, by simple extension, quasigeostrophic turbulence). Under a dual cascade, it is envisaged that from the scale at which energy and enstrophy are externally injected into a system, the enstrophy is conservatively cascaded to smaller scales through an enstrophy similarity range (i.e., transfer proceeds through every scale at the same rate), and energy is conservatively cascaded in the "inverse" direction to larger scales through an energy similarity range. The existence of two nonoverlapping similarity ranges, one for each of the two conserved quadratic quantities, is posited in order to satisfy the invariance of both the energy and the enstrophy.[1,2] The dual similarity range stationary spectrum, with a $k^{-5/3}$ slope in the energy similarity range and a k^{-3} slope in the enstrophy similarity range, follows directly from the dual cascade hypothesis and simple dimensional arguments and has been observed in 2-D neutral fluid flows.[7]

The dual cascade of 2-D Navier–Stokes turbulence has come to be a compelling paradigm for drift wave turbulence, a natural consequence of the near isomorphism of the Hasegawa–Mima[8] equation with the quasigeostrophic equation. The dual cascade is frequently invoked in a variety of drift wave models in order to infer the character and magnitude of fluctuations at the largest scales of a system, or to explain excitation at scales large compared to those of the driving instability. As such, the dual cascade is a key element of turbulence driven by electron temperature (η_e) modes.[9] More generally, it is assumed that the dual cascade is an element of spectral transfer for any system

 0899-8221/93/5(7)/2080/6/$6.00

possessing multiple quadratic invariants. Thus it figures prominently in the transfer dynamics of magnetohydrodynamic (MHD) turbulence.[10] As an example, specific properties of the dual cascade of three dimensional (3D) MHD have recently been invoked in order to predict ion heating rates in reversed field pinch discharges.[11] It is worth remarking that the dual cascade applies to spectral transfer in an inertial range. An inertial range may or may not exist in plasma turbulence, due to the nonlocalized nature of plasma driving sources and sinks. Nevertheless, inertial range transfer is a powerful and revealing characterization of the behavior of nonlinearities that are themselves conservative, and therefore would support an inertial range in the absence of dissipation.

The conventional view of the dual cascade process is based on analysis of spectral energy and enstrophy flow in 2-D Navier–Stokes turbulence for an infinite spectrum encompassing wave numbers from zero to infinity. For a spectrum with a single falloff rate of k^{-3} over its entire range $(0-\infty)$, Kraichnan[1] proved that there is a wave-number independent flow of enstrophy to high k, *and no flow of energy*. Such flow defines an enstrophy similarity range. Likewise, for a spectrum with a single falloff rate of $k^{-5/3}$, there is a wave-number independent flow of energy to low k, and no flow of enstrophy, defining an energy similarity range. In the k^{-3} spectrum, enstrophy is effectively injected at $k=0$ and removed at $k=\infty$, though no injection scale is specified in the analysis. In the $k^{-5/3}$ spectrum, energy is effectively injected at $k=\infty$ and removed at $k=0$. Both spectra are singular in the sense that there is no physically distinguishable scale that is not either zero or infinity, i.e., the injection scale and the minimum and maximum wave-number cutoffs are all either zero or infinity. Because these singular spectra are required for the proof, true similarity ranges can strictly be said to occur only in these rather extreme and amorphous spectra.

In fact, the standard stationary inertial range spectrum in 2-D turbulence is not one of the singular spectra analyzed by Kraichnan, but is forced or stirred at a finite scale k_{inj}^{-1}. It also has maximum and minimum wave numbers $k_{\max}$ and $k_{\min}$ corresponding to the smallest and largest inertial scales, typically set by dissipation and geometry. For drift wave turbulence, the spectrum is likely to be restricted to a very narrow range, perhaps encompassing no more than a single decade. For such finite spectra, it is crucial to account for the enstrophy carried in the energy flow and vise versa. Thus a self-similar inverse cascade of energy from k_{inj} to $k_{\min}$ results in the destruction of a portion of the enstrophy carried with the energy flow. Enstrophy is destroyed because it is proportional to the square of a spatial derivative (curl) of the flow, which necessarily becomes flatter as energy flows to large scale. This loss can be accommodated in an enstrophy conserving system only if enstrophy is created in some other part of the spectrum. The correct amount of enstrophy can be created if there is a self-similar cascade in the *reverse* direction (from k_{inj} to $k_{\max}$) of an appropriate fraction of the energy. Under this scenario, self-similar cascades of energy proceed in both directions, with accompanying nonconservative flows of enstrophy. The portion of energy flowing self-similarly in the reverse direction (to high k) is determined by the constraint of enstrophy conservation. Specifically, the enstrophy generated in the self-similar flow of energy to high k must equal the enstrophy destroyed in the self-similar flow of energy to low k. The above description applies to self-similar energy flow and the enstrophy carried with it. By symmetry, and in order to recover the results of Kraichnan's proof in the appropriate limits, there must also be a self-similar cascade of enstrophy, and it must proceed in both directions so as to yield zero net energy production from the accompanying nonconservative energy flows. This picture represents the simplest way to satisfy energy and enstrophy conservation, to reduce to Kraichnan's results in the appropriate limits, and to account for the changes that occur in one quantity when the other quantity is transferred between different scales.

In the present paper, spectral flows in numerical realizations of Hasegawa–Mima turbulence in a finite spectrum are measured and found to conform to this picture as formulated under simple dimensional analysis. The numerical results are obtained from spectral solution of the basic equation, with flow measurements achieved through direct evaluation of the triplet nonlinearity (of the power spectrum evolution equation). The numerical results indicate that significant nonconservative flows of enstrophy occur in both directions, and are consistent with enstrophy carried in self-similar energy flows proceeding in both directions. The reverse energy flow (self-similar energy flow to high k) generates sufficient enstrophy to compensate for the loss of enstrophy resulting from the proper energy flow (self-similar inverse cascade of energy to low k). Likewise, nonconservative flows of energy, consistent with self-similar flows of enstrophy in both directions are observed. The reverse enstrophy flow (to low k) destroys sufficient energy to compensate for the generation of energy by the proper enstrophy flow (to high k). For infinite spectra ($k_{\min}\to 0$, $k_{\max}\to\infty$), the dimensional analysis indicates that the reverse flows of energy and enstrophy vanish, while the nonconservative flows occur only in a narrow band near k_{inj}. Outside this band, the flows are self-similar and proceed according to the standard dual cascade hypothesis.

II. DIMENSIONAL ANALYSIS

Three constraints govern the flow of energy and enstrophy in a finite spectrum $k_{\min}<k_{\mathrm{inj}}<k_{\max}$. The flow configuration must account for changes in enstrophy (energy) due to the transfer of energy (enstrophy), energy and enstrophy must be conserved, and the flow configuration must reduce to Kraichnan's results in the proper singular spectrum limits. These constraints are most easily accommodated by dividing the flow of each invariant quantity (energy and enstrophy) into two components, a component that is transferred self-similarly (from which the correct self-similar transfer is recovered in the singular spectrum limits) and a locally (in wave-number space) nonconserved component representing the energy or enstrophy carried the self-similar flow of the other quantity.

At the injection scale, all inputted energy and enstrophy must be partitioned into either of these components, so that

$$E_0=E_c+E_N, \quad \Omega_0=\Omega_c+\Omega_N, \tag{1}$$

where E_0 is the injected energy, E_c is the amount of injected energy carried in self-similar energy flows, and E_N is the amount of injected energy in the nonconserving energy flows representing the energy carried by the self-similar *enstrophy* flows. Similar definitions apply to the inputted enstrophy Ω_0. Because enstrophy is mean-squared vorticity, the Fourier enstrophy $\Omega(k)$ (defined as the enstrophy of a Fourier mode of wave number k) of any flow with Fourier energy $E(k)$ is given by $\Omega(k)=k^2E(k)$. Thus the partition $E_0=E_c+E_N$, with E_N being the portion of injected energy carried by the self-similar enstrophy cascade, implies that

$$E_N=k_{\rm inj}^{-2}\Omega_c. \tag{2}$$

Likewise,

$$\Omega_N=k_{\rm inj}^2E_c. \tag{3}$$

Consider now the self-similar energy flow. Let E_p be the energy carried in a proper energy conserving cascade from $k_{\rm inj}$ to $k_{\rm min}$. A quantity of enstrophy $E_pk_{\rm inj}^2$ is carried in this cascade at the scale $k_{\rm inj}^{-1}$, but dwindles to $E_pk_{\rm min}^2$ as the energy reaches $k_{\rm min}$, a consequence of the smoother gradients associated with the large scale $k_{\rm min}^{-1}$. Obviously, the proper cascade of energy E_p between $k_{\rm inj}$ and $k_{\rm min}$ produces a net loss of enstrophy of magnitude $E_p(k_{\rm inj}^2-k_{\rm min}^2)$. This loss is the end result of the nonconservative enstrophy flow associated with the proper energy cascade. To assure overall conservation of enstrophy, enstrophy equal to the amount lost must be generated somewhere in the spectrum. This can occur if a portion of energy E_r cascades conservatively in the reverse sense from $k_{\rm inj}$ to $k_{\rm max}$. The steeper gradients associated with a flow of energy E_r at a scale $k_{\rm max}^{-1}$ results in a net production of enstrophy of magnitude $E_r(k_{\rm max}^2-k_{\rm inj}^2)$. Equating the net loss of enstrophy resulting from the proper cascade of energy with the net production of enstrophy resulting from the reverse cascade, the energies E_p and E_r are

$$E_p=E_c\frac{(k_{\rm max}^2-k_{\rm inj}^2)}{(k_{\rm max}^2-k_{\rm min}^2)}=E_c\frac{(1-I^2)}{(1-R^2)}, \tag{4}$$

$$E_r=E_c\frac{(k_{\rm inj}^2-k_{\rm min}^2)}{(k_{\rm max}^2-k_{\rm min}^2)}=E_c\frac{(I^2-R^2)}{(1-R^2)}, \tag{5}$$

where the total amount of conservatively cascaded energy $E_c=E_r+E_p$ is split into proper and reverse components, $I=k_{\rm inj}/k_{\rm max}$ and $R=k_{\rm min}/k_{\rm max}$. From these expressions it is obvious that as $k_{\rm max}\to\infty$ with $k_{\rm inj}$ remaining finite, $E_p\to E_c$ and $E_r\to 0$, yielding a unidirectional self-similar flow to low k, consistent with the dual cascade hypothesis for $k_{\rm inj}$ finite.

These arguments can be repeated for the conservative spectral flow of enstrophy. If Ω_p is the portion of enstrophy undergoing a proper self-similar cascade from $k_{\rm inj}$ to $k_{\rm max}$, energy carried in this flow decreases from its value $\Omega_pk_{\rm inj}^{-2}$ at the scale $k_{\rm inj}$ to $\Omega_pk_{\rm max}^{-2}$ at $k_{\rm max}$, i.e., a net amount of energy $\Omega_p(k_{\rm inj}^{-2}-k_{\rm max}^{-2})$ is lost in the conservative enstrophy transfer. Consequently, there must be a portion of enstrophy Ω_r reverse cascaded to $k_{\rm min}$, which produces a net increase of energy $\Omega_r(k_{\rm min}^{-2}-k_{\rm inj}^{-2})$. Equating the net loss and gain of energy in order to maintain energy conservation, the quantities of enstrophy cascaded in the proper and reverse directions are

$$\Omega_p=\Omega_c\frac{(k_{\rm min}^{-2}-k_{\rm inj}^{-2})}{(k_{\rm min}^{-2}-k_{\rm max}^{-2})}=\Omega_c\frac{(I^2-R^2)}{(1-R^2)}\frac{1}{I^2}, \tag{6}$$

$$\Omega_r=\Omega_c\frac{(k_{\rm inj}^{-2}-k_{\rm max}^{-2})}{(k_{\rm min}^{-2}-k_{\rm max}^{-2})}=\Omega_c\frac{(1-I^2)}{(1-R^2)}\frac{R^2}{I^2}, \tag{7}$$

where $\Omega_c=\Omega_p+\Omega_r$ is the total amount of enstrophy conservatively cascaded. Again, $k_{\rm min}\to 0$ with $k_{\rm inj}$ remaining finite implies that $\Omega_r\to 0$ and $\Omega_p\to\Omega_c$.

In the above discussions, the fraction of total injected energy that gets carried by the conservative enstrophy cascade E_N, is not specified relative to the fraction of energy going into the conservative energy cascade E_c. A reasonable hypothesis for this partition, based loosely on similarity and statistical homogeneity arguments, follows from

$$\Omega_c=E_ck_{\rm inj}^2. \tag{8}$$

Note that for an infinite spectrum ($k_{\rm max}=\infty$, $k_{\rm min}=0$) the ansatz of Eq. (8) applies solely to the proper cascades, i.e., spectral flows proceeding in opposite directions away from $k_{\rm inj}$; otherwise it applies to flows moving in both directions. Equation (8) fixes the ratio of conservative to nonconservative flow since the nonconservative energy flow is governed by the conservative enstrophy flow $E_n=\Omega_ck_{\rm inj}^{-2}$. Thus $E_n=E_c$. From these considerations, it is apparent that the nonconserved flows in either similarity range are significant. Even for the infinite spectrum ($k_{\rm max}=\infty$, $k_{\rm min}=0$, with $k_{\rm inj}$ finite), where the self-similar or conserved flows are entirely proper, the nonconserved flows remain, and they proceed in the reverse sense. The enstrophy in the nonconserved enstrophy flow decreases like k^{-2} as it cascades toward $k_{\rm max}=\infty$. Similarly, the energy in the nonconserved energy flow decreases like k^2 as it cascades toward $k_{\rm min}=0$. Consequently, the nonconserved flow is effectively confined to a region around $k_{\rm inj}$. Outside this region, flow is largely self-similar and proper, consistent with the dual cascade hypothesis.

Clearly, for finite spectra of limited extent, departures from the dual cascade picture are significant, arising from both the large nonconserved flows, as well as the reverse self-similar flows. The fact that reverse self-similar flows can be large is illustrated in Figs. 1 and 2, which plot the conserved energy and enstrophy flows [Eqs. (4)–(7)] as a function of the injection scale, $I=k_{\rm inj}/k_{\rm max}$ for $R=k_{\rm min}/k_{\rm max}=0.1$. In the limit $R\to 0$, $I\to 0$ ($R/I\to 0$), the spectrum is infinite and all of the conservatively cascaded energy and enstrophy flow in the proper directions. Away from this limit significant fractions of the injected energy and enstrophy can flow in the reverse directions. In particular, for $I>2^{-1/2}$ $(I+R^2)^{1/2}$, the reverse energy flow exceeds the proper energy flow. Thus, when $k_{\rm inj}$ is some-

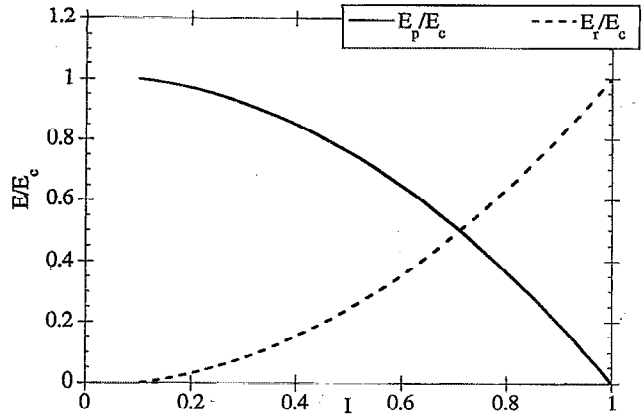

FIG. 1. The magnitude of the normalized self-similar energy flows in the proper and reverse directions as a function of $I=k_{inj}/k_{max}$. Normalization is with respect to the total energy carried in self-similar flows.

what more than halfway the distance from k_{min} to k_{max}, both enstrophy and energy flow primarily to high k, a result strikingly at variance with the standard dual cascade picture.

III. NUMERICAL ANALYSIS

In order to determine the extent to which spectral flow conforms to the heuristic description of the previous section, the Hasegawa–Mima equation is solved numerically and spectral flow is measured for several spectrum configurations. The Hasegawa–Mima equation

$$\frac{\partial}{\partial t}(1-\nabla_\perp^2\rho_s^2)\hat{\phi}+V_D\frac{\partial}{\partial y}\hat{\phi}+\rho_s^3C_s\nabla\hat{\phi}\times\mathbf{z}\cdot\nabla\nabla_\perp^2\hat{\phi}=0, \quad (9)$$

describes collective drift wave fluctuations supported by fluid ions and adiabatic electrons linked through quasineutrality. Here, $\hat{\phi}$ is the electrostatic potential, $V_D=(cT_e/eB)L_n^{-1}$ is the diamagnetic drift velocity representing $E\times B$ advection of the background density gradient, $\rho_s=(T_e/m_i)^{1/2}(eB/m_ic)^{-1}$ is the ion gyroradius evaluated at the electron temperature, and $C_s=(T_e/m_i)^{1/2}$ is the ion sound speed. Besides the diamagnetic drift, ion motion is governed by the polarization drift, which produces both the linear dispersion and the nonlinearity. Physically, the polarization drift nonlinearity represents $E\times B$ advection of the $E\times B$ flow vorticity and corresponds to the nonlinearity of 2-D Navier–Stokes turbulence. The assumption of adiabatic electrons ($n_e=\hat{\phi}$) eliminates linear instability, particle transport, and the enstrophy invariance-breaking $E\times B$ nonlinearity.[12] As is well known, the Hasegawa–Mima equation conserves both the energy $E=\int(|\hat{\phi}|^2+|\nabla\hat{\phi}|^2)\,dx\,dy$ and the enstrophy $\Omega=\int(|\nabla\hat{\phi}|^2+|\nabla^2\hat{\phi}|^2)dx\,dy$, and produces a condensation of energy at long wavelengths.[8] The latter is a manifestation that some energy undergoes an inverse cascade.

The Hasegawa–Mima equation is solved spectrally by numerically integrating the coupled ordinary differential equations for the time evolution of the amplitudes of the spatial Fourier series representation of $\hat{\phi}$. The wave-number space is truncated to a finite number of modes with 41×41 representing the largest spectral domain. Finite differencing in time is accomplished with a gear method. Spectral flow of energy is measured by determining the rate of spectral energy transfer.

$$T_k=-\rho_s^3C_s\,\mathrm{Re}\sum_{k'}\mathbf{k}\times\mathbf{k}'\cdot\mathbf{z}(k_\perp-k_\perp')^2\hat{\phi}_{k'}\hat{\phi}_{k-k'}\hat{\phi}_{k*}. \quad (10)$$

The quantity T_k represents the rate at which energy is deposited into or removed from the mode k by the nonlinear transfer. For $T_k<0$, energy is transferred from the mode to other parts of the wave-number spectrum, while for $T_k>0$, energy is deposited into the mode from other parts of the spectrum. Typically, T_k is summed over the modes in a band in wave-number space, thus giving a measure of the transfer rate into or out of the band. By examining the transfer rate for all bands, it is usually possible to track the flow of energy through the spectrum. Enstrophy flow is determined by measuring the rate of enstrophy transfer,

$$U_k=\rho_s^3C_s\,\mathrm{Re}\sum_{k'}\mathbf{k}\times\mathbf{k}'\cdot\mathbf{z}\,k^2(k_\perp-k_\perp')^2\hat{\phi}_{k'}\hat{\phi}_{k-k'}\hat{\phi}_{k*}. \quad (11)$$

Again, a band structure is utilized and the transfer into or out of all bands is observed.

Spectral transfer is examined under two spectrum configurations. In one, an initial spectrum of randomly phased finite amplitude fluctuations is allowed to relax to a quasi-equilibrium configuration, a state characterized by no net transfer in the time averaged sense. A large potential amplitude pulse is then applied at k_{inj} and the subsequent prompt transfer of energy and enstrophy is tracked throughout the spectrum. In a second configuration, transfer is monitored under conditions more akin to a driven/damped steady state. Here, the system is coherently forced at k_{inj} with dissipative sinks at k_{min} and k_{max}. After a steady state is established, a large pulse is again applied at k_{inj}, and the subsequent prompt transfer is observed. In

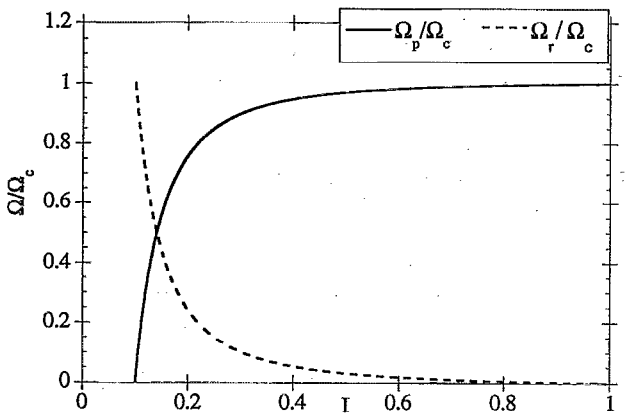

FIG. 2. The magnitude of the normalized self-similar enstrophy flows in the proper and reverse directions as a function of $I=k_{inj}/k_{max}$. Normalization is with respect to the total enstrophy carried in self-similar flows.

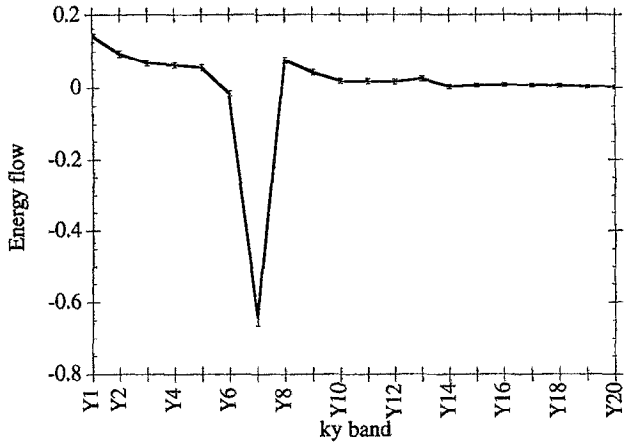

FIG. 3. Energy transfer rate for bands with k_y=const in numerical solutions of Hasegawa–Mima turbulence. Transfer is from a large perturbative pulse (at $k_{inj}=7$) applied to a quasiequilibrium spectrum. The error bars represent the standard deviation of the energy transfer rate about its mean value.

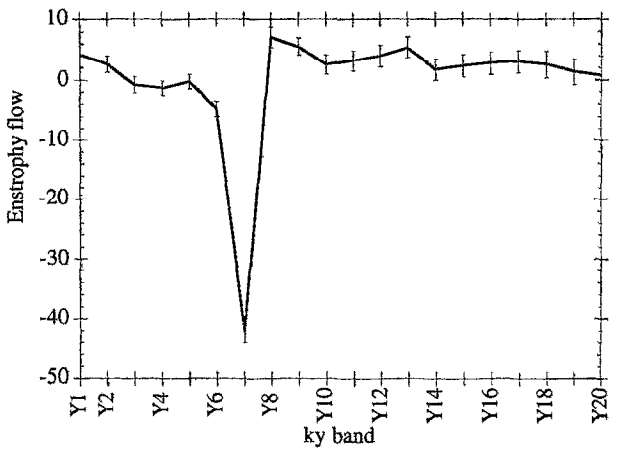

FIG. 4. Enstrophy transfer rate for the same case as Fig. 3.

both configurations, the prompt flow from the perturbative pulse is large compared to any preexisting flows. This ensures observation of the transfer characteristics of the nonlinearity, independent of the spatial arrangement or the relative strengths of the sources and sinks. This is necessary because in the steady state, the arrangement and strengths of the sources and sinks can dominate the flow pattern. Both spectrum configurations yield flow patterns that are essentially the same.

The behavior evident in the computational flow patterns is generally more complicated than the transfer of the simple picture developed in the previous section. Figure 3 shows the rate of energy transfer from a range of k_y=const bands spanning wave-number space. The transfer rate (vertical axis) is effectively an average obtained by summing discrete values of the instantaneous transfer rate over a period covering several nonlinear interaction times. The error bars denote the standard deviation from the mean value plotted. A large negative spike occurs at $k=k_{inj}$, indicating transfer out of the band with the large amplitude pulse. Positive values on either side of k_{inj} indicate that energy is transferred both toward k_{min} and k_{max}. The transfer is predominantly toward k_{min}; the steady rise in going to k_{min} is produced both by condensation and by the reverse flow of enstrophy to k_{min}. The flow of energy to high k diminishes as k increases, consistent with the destruction of energy carried in the proper cascade of enstrophy. The rate of decrease is roughly consistent with the k^{-2} scaling of the dimensional analysis. The run was terminated before there was any condensation of enstropy or energy at k_{max}.

The flow pattern for enstrophy is displayed in Fig. 4. Again enstrophy is seen to flow from k_{inj} in both directions. Here, however, more enstrophy flows toward high k than to low k. Condensation of enstrophy at k_{min} is clear evidence of a reverse enstrophy cascade but masks the nonconservative enstrophy flow associated with the proper energy cascade. The flow of enstrophy to high k is roughly constant, within errors bars, over the enstrophy similarity range. It is worth noting that self-similar (steady-state) cascade would produce zero net transfer into or out of any band. Here the flow is the transient response to the perturbative pulse and represents the propagation of the bulk of enstrophy in the pulse to high k, before condensation at k_{max}.

It is likely that differences between the results of Figs. 3 and 4 and the simple relations derived in the previous section stem both from limitations in the numerical work and the extreme simplicity of the dimensional analysis. In particular, the spectrum configuration is often arranged with k_{inj} as the geometric of k_{max} and k_{min}. Among other things, this choice makes the fractional proper cascaded energies and enstrophies comparable ($E_p/E_c \approx \Omega_p/\Omega_c$). Moreover, there is some evidence that this scale represents a natural break point for dual cascades in relaxing spectra with no forcing or perturbative pulse. Under such circumstances, k_{inj} is typically closer to k_{min} than it is to k_{max}. Consequently, there is considerable energy condensation at k_{min} before the transfer to high k reaches k_{max}. Because condensation produces spectrum changes that then affect transfer, it becomes difficult to track the upward transfer all the way to k_{max} once condensation has begun at k_{min}. A second limitation results from the analysis of transfer into or out of bands of constant k_x or k_y. This band structure permits the examination of anisotropies of the transfer rate. However, for the Hasegawa–Mima equation, the transfer is found to be isotropic, in which case the constant k_x or k_y band structure has the unwanted effect of potentially distorting measurement of transfer. For example, self-similar transfer of energy *within* a k_x=const band (from large k_y to small k_y) can decrease the enstrophy of the band, independent of the transfer occurring between bands. Another limitation arises from the effect of random fluctuations of the nonlinear interaction on the observed flow patterns. Even though the flow patterns are time averaged, some random component remains after averaging. Finally, the flow patterns represent the time average of a transient response to a perturbative pulse. The relaxation occurs on a time scale of several nonlinear interaction times, over

which the relaxation is monotonic. Hence, the direction of transfer under averaging would not differ from an instantaneous ensemble averaged direction. However, the time average integrates the response as it evolves, an effect that must be taken into account in interpreting the figures and making inferences about transfer in steady-state situations. For this reason, the transfer is generally not tracked after significant condensation has begun. Before condensation, the time average captures the propagation of the pulse in wave-number space effectively as a time exposure photograph.

Each of the above difficulties suggests improvements for future computational work. However, there is considerable agreement between the simple model and the results of this imperfect computational analysis. Certainly, the measured flow patterns are considerably altered from those envisioned in the standard dual cascade hypothesis. Energy and enstrophy are transferred away from k_{inj} in *both* directions. Moreover, there is evidence that the flow in a given direction away from k_{inj} is not completely self-similar. Also, runs with inertial ranges varied by over a factor of 3 indicate that the flow patterns tend toward the standard dual cascade configuration as the spectral range increases, i.e., the magnitude of the reverse (conservative) flows decreases relative to that of the proper flows.

IV. CONCLUSIONS AND DISCUSSION

The notion that energy and enstrophy respectively undergo self-similar cascades to long and short wavelengths in turbulence conserving these quantities has been shown to be appropriate only for infinite spectra ($k_{min}\to 0$, $k_{max}\to\infty$) away from the injection scale. Because enstrophy (energy) is carried in wave-number space by a self-similar energy flow (enstrophy flow) and increases or decreases depending on the direction of the flow, injected energy and enstrophy must flow from the injection in both directions. The energy lost in the proper self-similar cascade of enstrophy to high k is then compensated by the energy gained in a reverse self-similar cascade of enstrophy to low k. A similar statement applies to enstrophy lost and gained from proper and reverse energy cascades to low and high k, respectively. These constraints have been incorporated into simple scaling expressions from which the magnitude of proper, reverse, and the non- self-similar flows are obtained. The standard dual cascade results are recovered from these expressions in the limit $k_{min}\to 0$ and $k_{max}\to\infty$. These expressions therefore yield the dominant flow pattern of the infinite spectrum, a result often inferred from statistical mechanics arguments.

Large reverse energy flows are predicted when k_{inj} is near k_{max}. This case is instructive in reference to η_e turbulence,[9] where it has been asserted that there is an inverse cascade of energy to scales given by c/ω_{pe} (where ω_{pe} is the electron plasma frequency) from the smaller scales of collective excitation at ρ_e (the electron gyroradius). With driving already at very small scales, it is likely that dissipation occurs at scales only slightly above ρ_e, in which case Fig. 1 suggests that the dominant energy transfer would be toward short wavelengths, not the longer c/ω_{pe} scales. Because enstrophy also flows to high k, the dominant non- self-similar energy flow would also be toward high k.

This type of consideration clearly demonstrates that the practice of invoking a standard dual cascade for spectra with an inertial range bounded between limits not widely separated in wave-number space may not be valid. Even if damping is restricted to a region outside maximum and minimum cutoffs, the location of the scale at which fluctuations are excited within the region will play a significant role in the direction of energy flow. Moreover, because sources and sinks may in fact be distributed, with no true inertial range, determining the k space flow ultimately requires a knowledge of the spectrum. This, in turn, requires solution of the appropriate two-point equations, taking account of both the distributions of sources and sinks and the spectral properties of the nonlinearities.

ACKNOWLEDGMENT

This work was supported by U. S. Department of Energy Contract No. DE-FG02-89ER-53291.

[1]R. H. Kraichnan, Phys. Fluids **10**, 1417 (1967).
[2]C. E. Leith, Phys. Fluids **11**, 671 (1968).
[3]D. E. Newman, P. W. Terry, and P. H. Diamond, Phys. Fluids B **4**, 599 (1992).
[4]D. E. Newman, P. W. Terry, P. H. Diamond, and Y.-M. Liang, Phys. Fluids B **5**, 1140 (1993).
[5]Y.-M. Liang, P. H. Diamond, X. H. Wang, D. E. Newman, and P. W. Terry, Phys. Fluids B **5**, 1128 (1993).
[6]P. H. Diamond and H. Biglari, Phys. Rev. Lett. **65**, 2865 (1990).
[7]M. Gharib and P. Derango, Phys. D **37**, 406 (1989).
[8]A. Hasegawa and K. Mima, Phys. Rev. Lett. **39**, 205 (1977).
[9]W. Horton, B.-G. Hong, T. Tajima, and N. Bekki, Comments Plasma Phys. Controlled Fusion **13**, 207 (1990).
[10]A. Pouquet, U. Frisch, and J. Léorat, J. Fluid Mech. **77**, 321 (1976).
[11]N. Mattor, P. W. Terry, and S. C. Prager, Comments Plasma Phys. Controlled Fusion **15**, 65 (1992).
[12]P. W. Terry and W. Horton, Phys. Fluids **25**, 491 (1982).